Cell Reports

Article

Hippocampus-to-amygdala pathway drives the separation of remote memories of related events

Graphical abstract

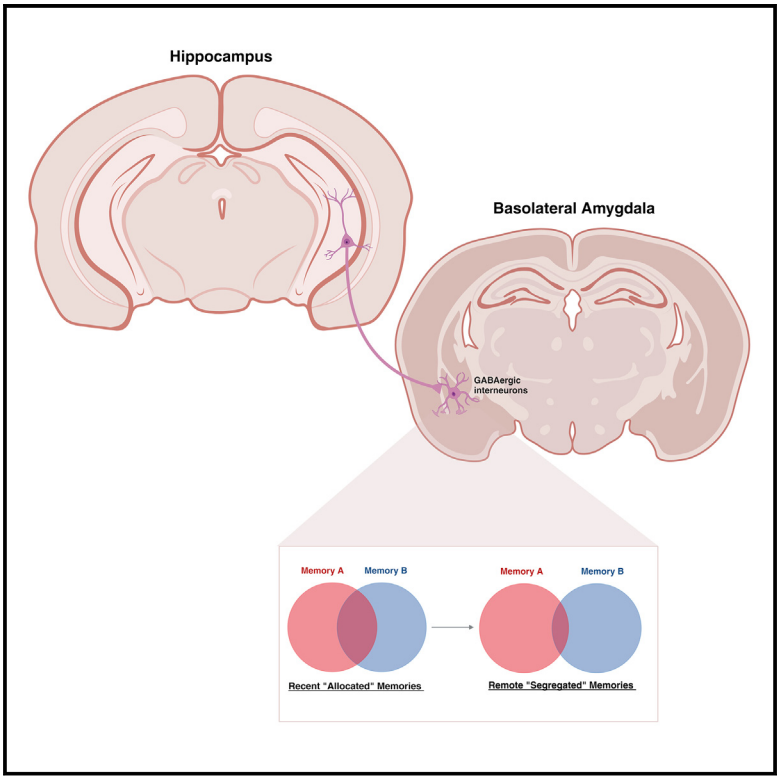

Highlights

- Hippocampus drives the pattern separation of fear memories in the amygdala
- Parvalbumin cells enable the separation of related fear memories in the amygdala
- Recent overlapped memories are transformed into segregated remote memories over time

Authors

Giulia Concina, Luisella Milano, Annamaria Renna, Eugenio Manassero, Francesca Stabile, Benedetto Sacchetti

Correspondence

benedetto.sacchetti@unito.it

In brief

Remembering closely related events poses a brain challenge. Each memory must retain its uniqueness while commonalities are recalled. Concina et al. found that hippocampal neurons guide amygdala inhibitory cells, separating overlapped memories. This insight aids understanding of memory segregation, which is compromised in disorders like schizophrenia and post-traumatic stress disorder.

Concina et al., 2024, Cell Reports *43*, 114151
May 28, 2024
https://doi.org/10.1016/j.celrep.2024.114151

CellPress

Cell Reports

CellPress
OPEN ACCESS

Article

Hippocampus-to-amygdala pathway drives the separation of remote memories of related events

Giulia Concina,[1,2] Luisella Milano,[1,2] Annamaria Renna,[1,2] Eugenio Manassero,[1] Francesca Stabile,[1] and Benedetto Sacchetti[1,3,*]

[1]Rita Levi-Montalcini Department of Neuroscience, University of Turin, 10125 Turin, Italy
[2]These authors contributed equally
[3]Lead contact
*Correspondence: benedetto.sacchetti@unito.it
https://doi.org/10.1016/j.celrep.2024.114151

SUMMARY

The mammalian brain can store and retrieve memories of related events as distinct memories and remember common features of those experiences. How it computes this function remains elusive. Here, we show in rats that recent memories of two closely timed auditory fear events share overlapping neuronal ensembles in the basolateral amygdala (BLA) and are functionally linked. However, remote memories have reduced neuronal overlap and are functionally independent. The activity of parvalbumin (PV)-expressing neurons in the BLA plays a crucial role in forming separate remote memories. Chemogenetic blockade of PV preserves individual remote memories but prevents their segregation, resulting in reciprocal associations. The hippocampus drives this process through specific excitatory connections with BLA GABAergic interneurons. These findings provide insights into the neuronal mechanisms that minimize the overlap between distinct remote memories and enable the retrieval of related memories separately.

INTRODUCTION

An important challenge for the brain is managing memories of distinct events that share common features or that occur in temporal proximity. The specificity of each memory should be preserved over time, and the common features of these experiences should be remembered. How this can be achieved is yet to be determined. Dysfunctions in the neural mechanisms underlying the distinction across highly similar memories form the core of several neuropsychiatric disorders, such as post-traumatic stress disorder (PTSD).

The hippocampus plays a pivotal role in the precise encoding and retrieval of distinct memories stemming from closely related experiences. This crucial function is elucidated through two processes: (1) pattern separation, aimed at minimizing overlap among pieces of information to facilitate their separate storage and retrieval, and (2) pattern competition, which allows the recall of stored information from partial cues.[1–7] Various neuronal processes within hippocampal circuits have been identified to support these functions.[7–9] Notably, recent studies indicate that when two distinct events occur in temporal proximity, such as within a 5–6 h interval, certain neurons activated by the initial event become engaged or "allocated" to encode the subsequent event in the hippocampus.[10–12] Overlapping neuronal ensembles establish connections between memories of related events, facilitating the capture of shared features across experiences.[12] A parallel mechanism has been observed in the basolateral amygdala (BLA),[13] a brain region that plays a crucial role in the formation and retrieval of fearful memories. Indeed, human studies have also demonstrated an interplay between the hippocampus and amygdala in the pattern separation of both episodic and emotional memories.[14,15]

However, the mechanism by which different memories within overlapping ensembles are preserved over time remains unknown. It is unclear whether remote memories of related events are stored partly within overlapping neurons or alternatively segregated into distinct neuronal populations. Further, the mechanisms to preserve the specificity of each memory over time are not understood. Here, we address these issues by analyzing the neuronal and behavioral features of two temporarily related memories at both recent and remote time intervals.

RESULTS

Memories of two events in temporal proximity are reciprocally linked at a recent time point but are independent at a remote time point

When memories of closely timed events are allocated to shared neuronal populations, the retrieval of one memory increases the likelihood of retrieval of the other.[10,11,13] Thus, we studied the process evolution over time by investigating whether the retrieval of one memory recruits neurons common to the other memory at either recent or remote time points when two fear events occur in temporal proximity (such as 6 h apart). To this end, we employed

the Daun02 inactivation method, which allowed inhibiting the activity of recall-induced neurons without affecting the neighboring cells.[16–19] c-Fos-lacZ transgenic rats carry a transgene in which the c-Fos promoter drives lacZ gene transcription and β-galactosidase (β-gal) expression. Induction occurs only in activated neurons that coexpress β-gal and c-Fos. When the prodrug Daun02 is administered post-memory recall, β-gal converts Daun02 into daunorubicin, which induces cell death (Figure 1A). c-Fos-lacZ transgenic rats were subjected to one auditory stimulus (conditioned stimulus [CS1]: pure tone, 15 kHz) paired with a painful unconditioned stimulus (US). Another different tone (CS2: pure tone, 1 kHz) was paired with the US. Rats could easily distinguish between the two tones (Figure S1). In accordance with previous studies,[13] pairings of CS1-US and CS2-US were separated by a brief (6-h) delay, allowing rats to learn two distinct yet temporally related events. Seventy-two hours after the learning session, CS1 was presented to reactivate recent memory of CS1 (CS1 memory reactivation) (Figure 1B). To selectively trigger the reactivation of CS1 memory while minimizing interference associated with contextual cues, CS1 was presented in a novel environment. The presentation of CS1 in this new context resulted in a substantial increase in freezing behavior (indicative of defensive responses) across all rats (Figures S2A). Ninety minutes later, Daun02 or vehicle was injected into the BLA (Figures S3A and S3B). The assessment of memory retention for CS2 (i.e., the memory not explicitly reactivated, CS2 memory retention) and CS1 (CS1 memory retention) was conducted 3 and 5 days later, respectively, in distinct new environments. During CS2 memory retention, Daun02-treated rats exhibited lower freezing compared to vehicle-treated rats (Figure 1C). Furthermore, in an additional group of rats, Daun02 administration in the absence of CS1 reactivation did not impact freezing to CS2 (Figure 1C), confirming that amnesia, when present, was specifically induced by Daun02-mediated inactivation of neurons activated during CS1 memory recall. Finally, during the CS1 memory retention test, Daun02-treated rats showed reduced freezing (Figure 1D), aligning with the notion that Daun02 injection impaired neurons associated with CS1 memory. Ninety minutes after the CS1 memory retention test, rats were sacrificed, and the number of cells expressing β-gal in the BLA was quantified. In comparison to vehicle-treated rats, the Daun02-treated group exhibited a reduced number of cells expressing β-gal (Figures S4A and S4B), thereby confirming the efficacy of the Daun02 manipulation.[17–19] We further assessed the correlation between the percentage of cells expressing β-gal and freezing responses to CS1 within each group (Figure S4C), revealing no significant correlation. This lack of correlation may be attributed to the fact that defensive behavior is likely regulated by a complex brain network. Similar results were obtained by counterbalancing tones (Figure S5A).

Taken together, these data are consistent with previous findings demonstrating that when memories of two events occurred in temporal proximity (like the 6-h group), CS1 memory recall recruited neurons necessary for CS2 memory.[10–13]

To ascertain that the observed effects were specifically linked to two distinct yet temporally related events, we compared the data obtained in Daun02-treated rats in the 6-h group with those of two additional rat groups. In one group, rats learned about a continuous fear event (i.e., CS1-US and CS2-US pairings occurred in a single continuous trial with a 0-min intertrial interval; 0-min group). In the second group, two temporally distant events were presented (CS1-US and CS2-US pairings were separated by a long 7-day interval; 7-day group). Seventy-two hours after the learning session, CS1 was presented to reactivate CS1 recent memory in all groups (Figure S2B). Ninety minutes later, Daun02 was injected, and the retention of CS2 and CS1 was assessed 3 and 5 days later, respectively. During CS2 memory retention, the freezing of rats in the 0-min and 6-h groups was lower than that in 7-day group (Figure 1E). Conversely, all groups displayed low freezing to the subsequent CS1 memory retention test (Figure 1F) and a low percentage of cells expressing β-gal after CS1 memory retention trial (Figures S4B and S4C).

Next, we performed similar experiments at a remote time interval, i.e., 3 weeks after learning (Figure 1G). At this time point, CS1 was presented (CS1 memory reactivation), and all rats displayed high freezing (Figures S2C and S2D). 90 min later, Daun02 or vehicle was injected into the BLA (Figures S3C and S6). The retention of CS2 and CS1 was assessed 3 and 5 days later, respectively. Unexpectedly, during CS2 memory retention, the freezing of Daun02-treated rats was similar to that of vehicle-treated rats (Figure 1H). Conversely, during the subsequent CS1 memory retention test, freezing of Daun02-injected rats was lower than in vehicle-treated rats (Figure 1I). Thus, the inactivation of CS1 recall-induced neurons at remote time points did not affect the retention of CS2 remote memories. Similar results were obtained by counterbalancing tones (Figure S5B). Moreover, during the CS2 memory retention test, Daun02-treated rats in the 6-h group displayed freezing higher than the 0-min group and similar to the 7-day group (Figure 1J). All groups displayed amnesia to CS1 (Figure 1K), and a low percentage of cells expressing β-gal after the CS1 memory retention trial (Figure S6). Thus, at remote time points, the memories of two different but temporally related events are separate and independent, similar to the memories of two temporally distant events, while memories of CS1 and CS2 occurring in a unique continuative event continue to be linked.

The auditory cortex, particularly the higher-order auditory cortex, plays a key role in the storage and retrieval of remote auditory memories.[20–22] Therefore, in the 6-h group, we retrieved the CS1 remote memory and injected Daun02 into the auditory cortex (Figures S7A and S7B). During the CS2 remote memory retention test, freezing was similar between Daun02-and vehicle-injected rats (Figures S7C and S7D), suggesting that CS2 memory was also unaffected by CS1 remote memory retrieval at the cortical level.

Another feature of allocated auditory fear memories is that the extinction of one recent memory also extinguished the other one.[13] Thus, we investigated whether memories of temporarily related events could extinguish each other at either recent or remote time points. Wild-type rats were trained at 0-min, 6-h, and 7-day intervals (Figure 2A). CS1 recent memory was extinguished by repeatedly presenting CS1 in the absence of US 72 h after learning (Figure 2B). The following day, we assessed CS2 memory retention. Freezing to CS2 decreased in the 0-min and 6-h groups but not in the 7-day group (Figure 2C).

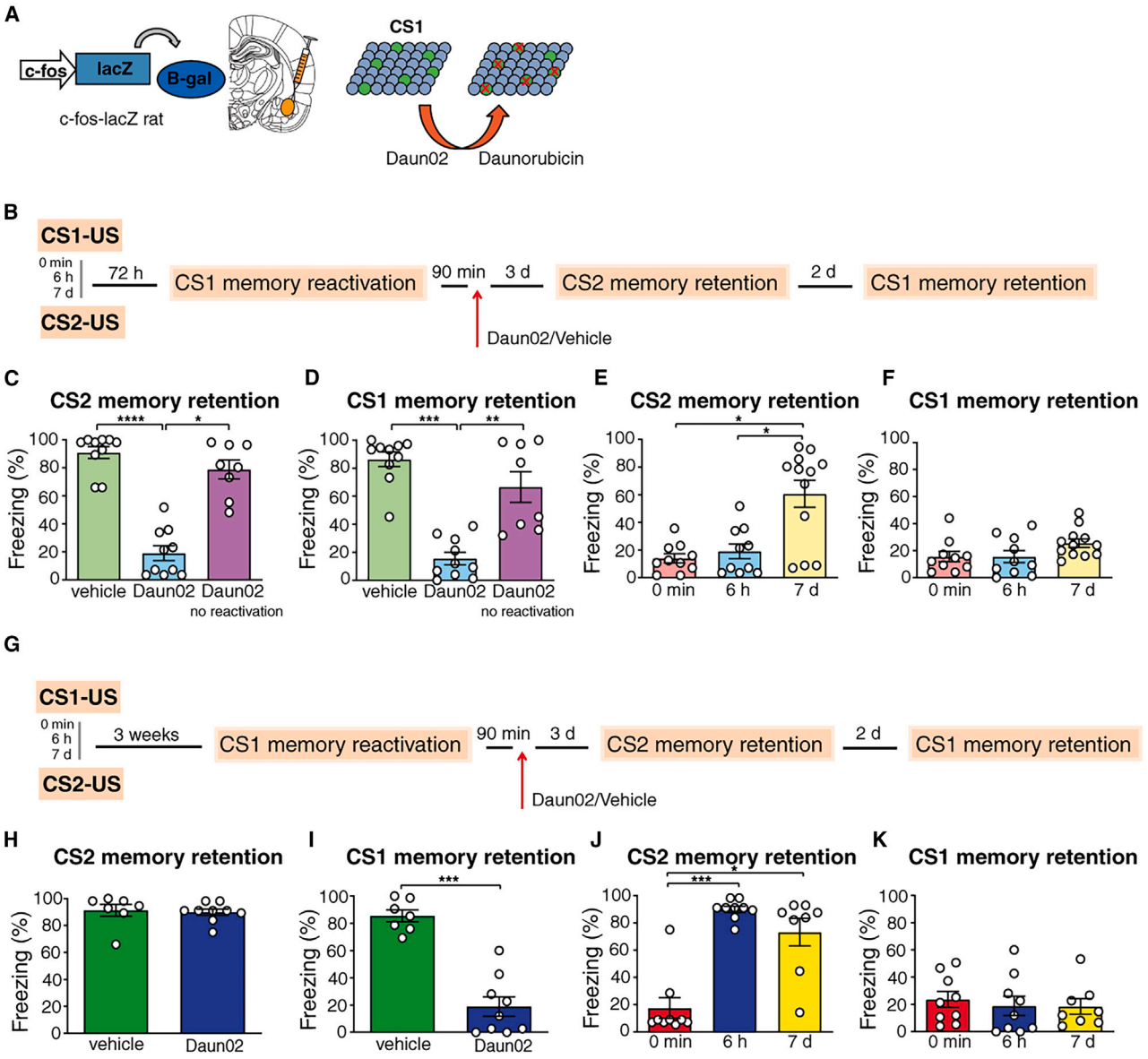

Figure 1. The targeted inhibition of neurons activated during CS1 memory reactivation disrupts the retention of recent memories to CS2 while leaving unaffected the retention of CS2 remote memories

(A) Schematic of Daun02-inactivation technique in c-Fos-lacZ transgenic rats.

(B) CS1-US and CS2-US occur at 0-min, 6-h, or 7-day delay. The recent memory is reactivated by representing CS1 72 h after the initial learning. CS1, conditioned stimulus1; CS2, conditioned stiumulus2; US, unconditioned stimulus.

(C) In the 6-h group (n = 10), Daun02-injected rats display lower freezing to CS2 than those receiving vehicle (n = 10) or Daun02 without CS1 presentation (n = 8) (H = 19.80, $p < 0.0001$).

(D) A similar result was observed during the subsequent presentation of CS1 (H = 17.83, $p = 0.0001$).

(E) Freezing to CS2 in 0-min (n = 10) and 6-h (n = 10) groups is lower than in the 7-day (n = 12) group (Kruskal-Wallis and Dunn test, H = 10.13, $p = 0.0063$).

(F) All three groups showed low freezing to CS1 (H = 5.75, $p = 0.056$).

(G) Similar experiments were repeated 3 weeks after learning to assess remote memories.

(H) At 3 weeks, in the 6-h group (n = 9), Daun02-injected rats display freezing to CS2 like the vehicle-injected rats (n = 7) (Mann-Whitney, U = 21.50, $p = 0.308$).

(I) On the contrary, in the presence of CS1, Daun02-injected rats display lower freezing than the vehicle-injected rats (U = 0 $p = 0.0002$).

(J) At 3 weeks, the 6-h group (n = 9) displays freezing to CS2 like the 7-day group (n = 8) but higher than the 0-min group (n = 9) (H = 16.76, $p = 0.0002$).

(K) In the presence of the CS1, all groups showed low freezing (H = 0.80, $p = 0.669$).

Data are means ± SEM. *$p < 0.05$, **$p < 0.01$, and ***$p < 0.001$.

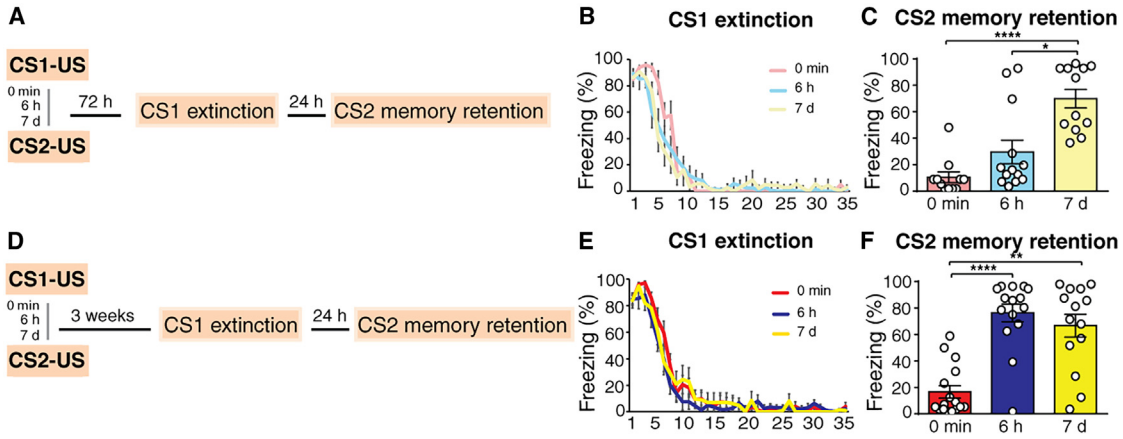

Figure 2. The extinction of CS1 memory extinguished CS2 recent memories while leaving unaffected CS2 remote memories

(A) Schematic diagram for evaluating CS2 memory following CS1 extinction in wild-type rats at a recent time point (72 h after learning).

(B) CS1 memory was extinguished by repeatedly presenting the CS1 in wild-type rats conditioned at 0-min (n = 11), 6-h (n = 13), or 7-day (n = 12) delay.

(C) CS1 extinction decreases CS2 freezing in 0-min and 6-h groups but not in 7-day group (H = 19.42, $p < 0.0001$).

(D) A similar experiment was repeated at a remote time point (3 weeks after learning).

(E) Fear extinction curves obtained by repeatedly presenting CS1 at remote (3 weeks) time point in rats conditioned at 0-min (n = 16), 6-h (n = 15), or 7-day (n = 14) delay.

(F) At 3 weeks, CS1 extinction extinguishes CS2 memory in 0-min but not in 6-h or 7-day groups (H = 20.63, $p < 0.0001$).

Data are means ± SEM. *$p < 0.05$, **$p < 0.01$, ***$p < 0.001$, and ****$p < 0.0001$.

We aimed to verify that the CS2 freezing decrease was specifically attributed to the extinction of the related CS1 memory and not to the mere repeated presentation of a tone. Thus, in an additional group, rats learned only the CS2-US association and were repeatedly presented with the 15-kHz tone (which acted as the CS1 in the previous groups). This procedure did not decrease freezing to CS2 (Figure S8A).

We repeated a similar experiment with CS1 extinction and CS2 memory tests performed 3 weeks after learning (Figure 2D). After CS1 remote memory extinction (Figure 2E), freezing to CS2 in the 6-h group was higher than in the 0-min group and similar to that in the 7-day group (Figure 2F). This result was not attributed to a change in susceptibility to fear extinction at more remote time points because the extinction curves were similar across recent and remote time points (Figures 2B and 2E), and CS1 remote memory was extinguished effectively (Figure S8B). We obtained similar results by counterbalancing the tones (Figure S8C).

Thus, memories of temporarily related events were reciprocally linked at a recent time point such that the recall (or extinction) of one memory led to the recall (or extinction) of another. However, memories of these events are functionally independent and refractory to the modification of the other at a remote time point.

Two temporarily related but distinct events are allocated to overlapping neuronal populations at a recent time point and to mostly separate neuronal populations at a remote time point.

Shortly after two auditory fear events occurring closely in time, overlapping populations of excitatory cells are allocated to both memories in the BLA.[10–13] Therefore, we examined the populations of excitatory neurons that underlie the recall of CS1 and CS2 memories at recent and remote time points in the BLA. To label neurons activated by each memory recall task, we injected an inducible, activity-dependent virus cocktail of adeno-associated virus AAV9-c-Fos-tTA and AAV9-TRE-enhanced yellow fluorescent protein (EYFP) viruses, which labeled the neurons expressing the immediate-early gene c-Fos in a doxycycline (Dox)-dependent manner (Figures 3A and 3B).[23,24] To specifically examine excitatory cells, brain sections were incubated with anti-EYFP, anti-c-Fos, and anti-CamKII (a marker for excitatory cells) antibodies. Rats received CS1-US and CS2-US pairings separated for 6 h on a Dox-on diet. Seventy hours later, CS1 was presented on the Dox-off diet to label neurons activated by CS1 recall with EYFP. Subsequently, the rats were fed a Dox-on diet, administered CS2 (Figures 3C and 3D), and perfused. Neurons activated by CS2 memory recall were detected by immunohistochemistry for endogenous c-Fos. The presentation of CS1 resulted in a minimal percentage of activated excitatory cells expressing EYFP in rats under the Dox-on diet (approximately 2% labeled cells, Figure S9). Conversely, in rats following the Dox-off diet, the percentage of activated excitatory cells expressing EYFP, including background positive cells, was notably elevated (Figures 3E and 3G). CS2 presentation led to endogenous c-Fos expression (Figures 3E and 3H). Critically, the percentage of excitatory neurons activated by both CS1 and CS2 was significantly higher than that expected by chance (Figures 3E and 3I).

We repeated a similar analysis by reactivating CS1 and CS2 memories 3 weeks after learning. Freezing to CS1 and CS2 was similar at the remote and recent intervals (Figure 3D). However, significantly fewer excitatory neurons were activated only by CS1 at the remote time point than that in the recent time point (Figures 3F and 3G). Conversely, we observed no difference in the percentage of neurons activated only by CS2 (Figures 3F and 3H). Critically, fewer neurons were activated by both CS1 and CS2 at the remote versus recent time point (Figure 3I). To further depict the differential activation of neurons between recent and remote intervals, we analyzed the ratio of EYFP and

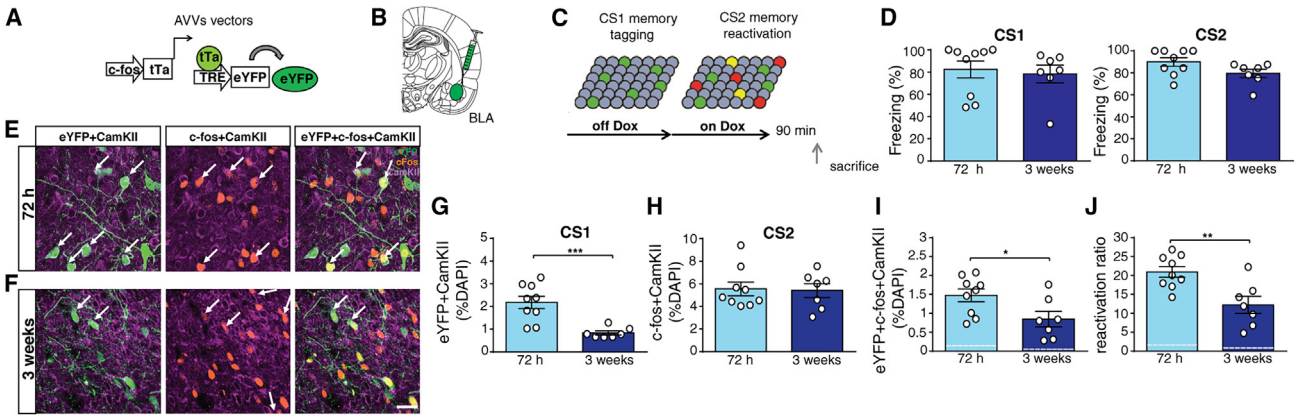

Figure 3. Memories of related events demonstrate higher overlapped neuronal ensemble at recent than at remote time points

(A and B) Viruses are injected into the BLA in wild-type rats on a doxycycline (Dox) diet.

(C) Rats feed on Dox-off diet during CS1 presentation (green). Next, they feed on Dox-on diet, and CS2 is presented (red).

(D) Freezing to CS1 (left) and CS2 (right) was similar between rats tested at recent (n = 9) and remote (n = 7) time points (Mann-Whitney, CS1, U = 20, p = 0.238; CS2, U = 16.50, p = 0.113).

(E and F) To specifically examine excitatory cells, brain sections were incubated with anti-EYFP, anti-c-Fos, and anti-CamKII (a marker for excitatory cells) antibodies. Confocal images of excitatory neurons expressing EYFP, c-Fos, or both at recent (E) or remote (F) time points. Arrows indicate recall-activated neurons. Scale bar, 20 μm.

(G) Neurons activated by the only CS1 presentation (EYFP$^+$CS1) are calculated as total EYFP$^+$ cells minus EYFP$^+$c-Fos$^+$ cells. EYFP$^+$CS1 cells decrease more in the remote (n = 7) than in the recent (n = 9) time point (Student's t test, $t_{(14)}$ = 4.19, p = 0.0009).

(H) Neurons activated by the only CS2 presentation (c-Fos$^+$CS2) are calculated as total c-Fos$^+$ cells minus EYFP$^+$c-Fos$^+$ cells. c-Fos$^+$CS2 expression is similar across time intervals ($t_{(14)}$ = 0.17, p = 0.866).

(I) EYFP$^+$c-Fos$^+$ cells decrease more in remote than in recent time points ($t_{(14)}$ = 2.38, p = 0.031). The percentage of overlapped neurons is over chance levels (dashed lines) in the recent ($t_{(8)}$ = 9.03, p < 0.0001) and remote ($t_{(6)}$ = 3.94, p = 0.0076) time points.

(J) The reactivation rate (EYFP$^+$c-Fos$^+$/c-Fos$^+$) decreases more in remote than in recent time points ($t_{(14)}$ = 3.42, p = 0.0041). The percentage of overlapped ensemble is over chance levels in both recent ($t_{(8)}$ = 14.15, p < 0.0001) and remote time points ($t_{(6)}$ = 5.20, p = 0.002).

Data are means ± SEM. *p < 0.05, **p < 0.01, and ***p < 0.001.

c-Fos double-positive cells among c-Fos$^+$ cells (EYFP$^+$c-Fos$^+$/c-Fos$^+$).[25] A significant difference between the recent and remote time points was observed (Figure 3J). Despite being lower than that at a recent time point, the percentage of overlapping neuronal populations at a remote time point was significantly higher than chance levels (Figures 3I and 3J), e.g., remote memories still maintained a significant population of overlapping neurons.

Taken together, the percentage of overlapping neuronal ensembles activated by both CS1 and CS2 significantly decreased at remote time points, where the most distinct neuronal populations underlie CS1 and CS2 memories. At the behavioral level, the disruption of neurons activated by CS1 remote recall did not affect CS2 memory, and CS1 extinction did not extinguish CS2 memory. Therefore, this process reduced the interference across related memories. Meanwhile, the neuronal overlap persisting at a remote time point may allow the maintenance of information on the shared features of related experiences.

Parvalbumin-positive interneurons within the BLA are necessary to form separate remote memories

Next, we investigated cellular mechanisms that may underlie the formation of independent remote memories. Upon or shortly after learning two contiguous events, the increase in the excitability of excitatory neurons could bias the encoding of a subsequent memory to neurons that encode the first memory.[10–13,26] Because gamma-aminobutyric acid (GABA)-ergic interneurons inhibit excitatory neurons, we hypothesized that inhibitory neurons may be activated to circumscribe the shared population of excitatory neurons across related memories.

In the BLA, a large proportion of inhibitory synapses onto excitatory neurons are formed by interneurons that express the calcium-binding protein parvalbumin (PV).[27,28] Therefore, we analyzed the activity of PV-positive cells in the 0-min, 6-h, and 7-day groups as well as in naive rats. In the 0-min group, the learning trial occurred in only one session, whereas the other groups underwent two different learning sessions. Thus, in the 0-min group, the first trial was repeated twice, 6 h apart, like that in the 6-h group. The animals were euthanized 90 min after the last learning session, and the number of PV cells expressing the c-Fos protein was analyzed. c-Fos expression has often been used as a marker of neuronal activity in excitatory and inhibitory neurons.[29,30] In all conditioned groups, c-Fos expression was higher than in naive animals (Figures 4A and 4B). Critically, the number of PV cells also expressing c-Fos was higher in the 6-h group than in the other groups (Figures 4A and 4C).

To investigate whether PV cells are involved in the formation of separate remote memory, we injected an AAV encoding the Cre-dependent hM4D(Gi) inhibitory designer receptor exclusively activated by designer drugs (DREADD) (AAV5-hSyn-DIO-hM4D(Gi)-mCherry) into the BLA of PV-Cre rats (Figure 4D).[31,32] Cre-dependent hM4D(Gi)-mCherry was specifically expressed in PV-positive BLA neurons (Figure 4E). Another group received the control AAV5-hSyn-DIO-mCherry. Both groups underwent

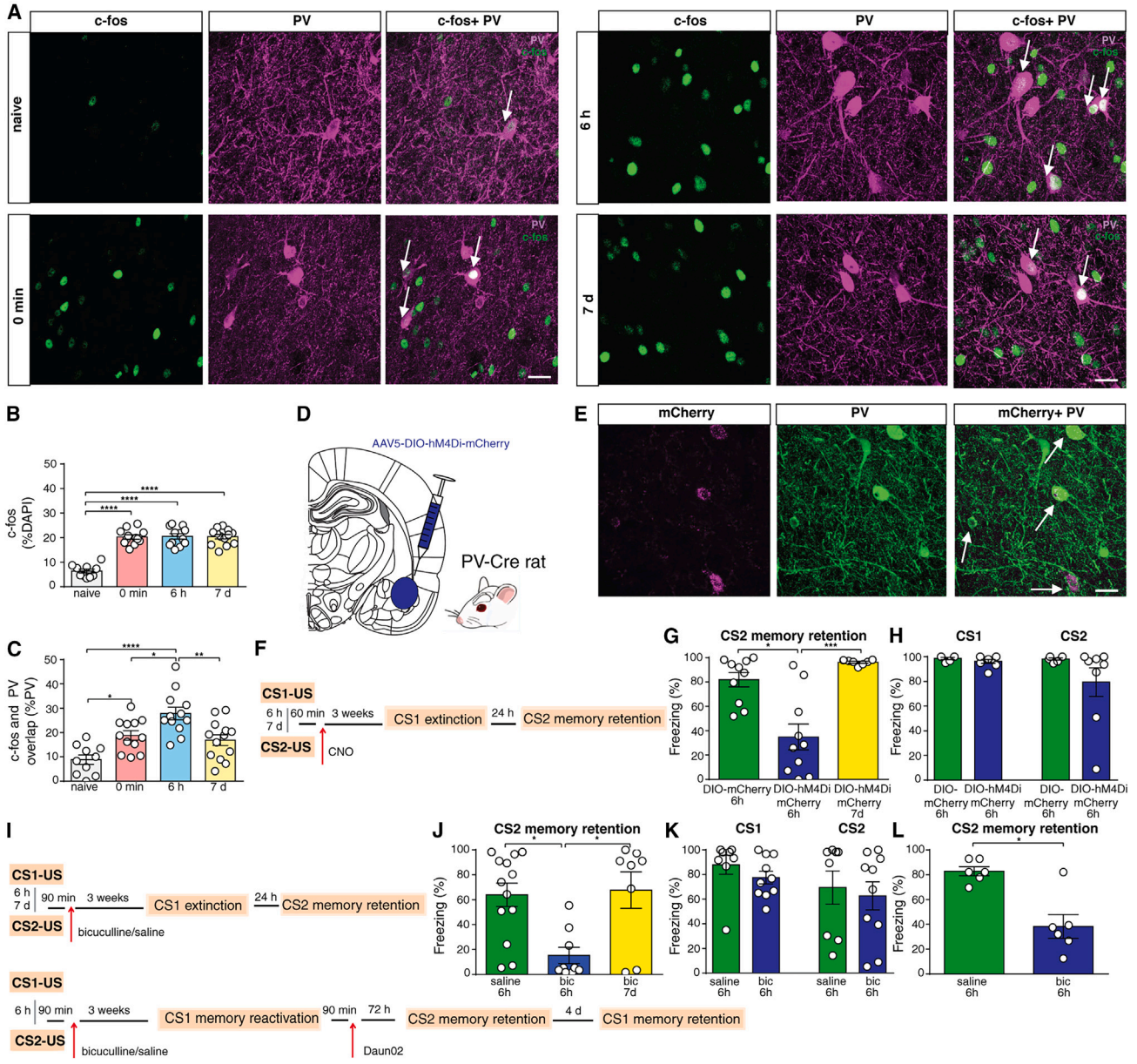

Figure 4. PV cells in the BLA are necessary for the formation of separate remote memories

(A) Costaining of parvalbumin (PV) and c-Fos in the BLA of naive rats and those conditioned with CS1-US and CS2-US at 0-min, 6-h, and 7-day delay. Arrows indicate PV-positive and c-Fos-positive cells. Scale bar, 20 μm.

(B) c-Fos expression is lower in naive (n = 10) rats than in other groups (one-way ANOVA and Tukey post-test, $F_{(3,43)} = 51.04$, $p < 0.0001$). No differences are observed among the 0-min (n = 12), 6-h (n = 12), and 7-day (n = 13) groups.

(C) PV-positive cells that also express c-Fos are higher in the 6-h group than in other groups ($F_{(3,43)} = 11.79$, $p < 0.0001$).

(D) Expression of AAV5-hSyn-DIO-hM4D(Gi)-mCherry in BLA PV neurons of PV-Cre rat.

(E) Dual-labeled hM4D(Gi)-mCherry/PV neurons are indicated with white arrows. Scale bar, 20 μm.

(F) Experimental design.

(G) CS1 extinction decreases CS2 memory in DIO-hM4D(Gi)-mCherry rats (n = 10) compared with DIO-mCherry rats (n = 10) and DIO-hM4Di-mCherry rats conditioned at a 7-day interval (n = 7) (Kruskal-Wallis and Dunn post hoc, H = 14.78, p = 0.0006).

(H) In the absence of CS1 extinction, CS1 and CS2 remote memories are similar between DIO-hM4D(Gi)-mCherry (n = 8) and DIO-mCherry (n = 6) rats (Mann-Whitney, CS1, U = 14.50, p = 0.208; CS2, U = 13.00, p = 0.165).

(I and J) Bicuculline injection into BLA decreases freezing to CS2 after CS1 extinction (n = 9) compared to saline-injected rats (n = 13) and bicuculline-injected rats conditioned at a 7-day interval (n = 8) (H = 9.93, p = 0.007).

(legend continued on next page)

CS1-US pairing, followed by CS2-US pairing 6 h later. Clozapine-N-oxide (CNO) was injected intraperitoneally 60 min after CS2-US learning to inactivate PV cells during the memory consolidation process at a time point at which PV activity was increased in the 6-h group. 3 weeks later, CS1 remote memory was extinguished (Figure 4F). All groups demonstrated a similar extinction curve (Figure S10A). The subsequent day, we assessed CS2 memory retention. Freezing to CS2 was lower in the DIO-hM4D(Gi)-mCherry group than that in the DIO-mCherry group (Figure 4G). In an additional group, in which DIO-hM4D(Gi)-mCherry PV-Cre rats were conditioned to CS1-US and CS2-US separated by 7 days, CS2 memory was unaffected by CS1 extinction (Figure 4G).

We repeated the previous experiment without extinguishing the CS1 memory, i.e., by presenting only a few CS1 and assessing CS2 memory the following day. No differences were detected between groups (Figure 4H). Thus, the decrease in freezing to CS2 in DIO-hM4D(Gi)-mCherry PV-Cre rats in the 6-h group was selectively attributed to the extinction of CS1 memory, i.e., the two memories were still reciprocally linked[13]

To further verify that GABAergic neurotransmission in BLA is involved in the formation of separate remote memories of temporally related fear events, we injected bicuculline, a selective GABAa receptor inhibitor, into the BLA (Figures S10B and S10C) of wild-type rats 90 min after learning. Three weeks later, CS1 memory was extinguished (Figure S10D), and CS2 memory was assessed (Figure 4I). Compared with saline-injected rats, freezing to CS2 decreased in the 6-h group but not in the 7-day group (Figure 4J). Importantly, bicuculline did not affect CS1 or CS2 memory retention in the absence of CS1 extinction (Figure 4K). Finally, bicuculline (or saline) was injected into the BLA of c-Fos-lacZ transgenic rats 90 min after learning. Three weeks later, we reactivated the CS1 memory and injected Daun02 to block CS1-memory-related neurons. During the CS2 memory retention test, rats that received bicuculline displayed a weaker freezing than those that received saline (Figures 4I, 4L, and S10E).

These data identified an important function of GABAergic cells within the BLA in memory processes. Chemogenetic inactivation of PV cells or GABAergic neurotransmission blockade did not affect the retention of individual remote memories but prevented the segregation of each remote memory into a functionally independent memory such that the two memories remained reciprocally linked. This function was related to the formation of separate memories of temporally related events but not separate memories of events that occurred 7 days apart.

Hippocampus regulates the segregation of remote memories through axons terminating directly onto the GABAergic interneurons of the BLA

The precise encoding and retrieval of distinct memories of related events are the central functions of the hippocampus. The hippocampus performs this function through a process termed pattern separation, which allows the conversion of highly related overlapping inputs into non-overlapping distinct outputs.[1–7] This process may reduce interference across related memories, ensuring that other related memories are not recalled during the retrieval of a specific memory and that the specificity of memories is maintained over time.[1–7] Therefore, we investigated whether the hippocampus is involved in reducing the overlap between remote auditory fear memories and its underlying mechanism.

c-Fos-lacZ transgenic rats were subjected to two learning events separated by 6 h (Figure 5A). Ninety minutes later, Daun02 (or vehicle) was administered into the dorsal hippocampus (Figures S11A) to inactivate the neurons specifically activated by these events. Three weeks later, the remote CS1 memory was extinguished (Figure 5B), and CS2 memory was assessed. Compared to the control animals, freezing to CS2 was lower in Daun02-injected animals (Figure 5C). Animals that received Daun02, in which CS1 was not extinguished, displayed high freezing to CS2 (Figure 5C). Thus, inactivating the dorsal hippocampus prevented the segregation of the two remote memories.

Thus far, CS1-US and CS2-US pairings have occurred in two distinct environments to differentiate between the two learning events. Next, we sought to determine whether hippocampal participation was related to the management of distinct contextual memories or distinct episodic fear memories regardless of the learning environment. We performed a similar experiment with CS1-US and CS2-US pairings in the same context (Figure 5D). During CS1 extinction trials, control rats exhibited a slower extinction curve. Nevertheless, ultimately, both groups effectively extinguished CS1 memory (Figure 5E). During CS2 memory retention, freezing to CS2 was lower in Daun02-injected animals than in control animals (Figure 5F). Therefore, the dorsal hippocampus plays a key role in ensuring that remote memories of events in temporal proximity are stored as distinct memories also when the two events occurred in the same context.

Next, we investigated whether the hippocampus interacts with the BLA to form distinct remote memories. We injected a retrograde AAVrg-hSyn-hM4D(Gi)-mCherry into the BLA to label and manipulate the hippocampal excitatory axons that terminated in the BLA (Figures 6A and 6B). The control group received AAVrg-hSyn-mCherry. Both groups underwent two auditory fear learning sessions separated by 6 h. Ninety minutes later, CNO was injected into the hippocampus to inactivate the excitatory neurons that projected to the BLA. Because most afferents to the BLA exited the ventral hippocampus,[33,34] CNO was administered to the ventral hippocampal region (Figures 6C and 6D). Three weeks later, CS1 was extinguished (Figure 6E), and CS2 memory was assessed. Compared to AAVrg-mCherry animals, AAVrg-hM4D(Gi)-mCherry animals froze to CS2 significantly less (Figure 6F). We did not find any effects in the absence of

(K) In the absence of CS1 extinction, CS1 and CS2 memories are similar between bicuculline- (n = 10) and saline-injected rats (n = 8) (CS1, U = 22.00, p = 0.115; CS2, U = 32.00, p = 0.498).

(L) In *c-Fos*-lacZ rats, Daun02 injection after CS1 memory recall decreases freezing to CS2 in bicuculline-injected rats (n = 6) compared with saline-injected rats (n = 6) (U = 3.00, p = 0.0152).

Data are means ± SEM. *p < 0.05, **p < 0.01, and ***p < 0.001.

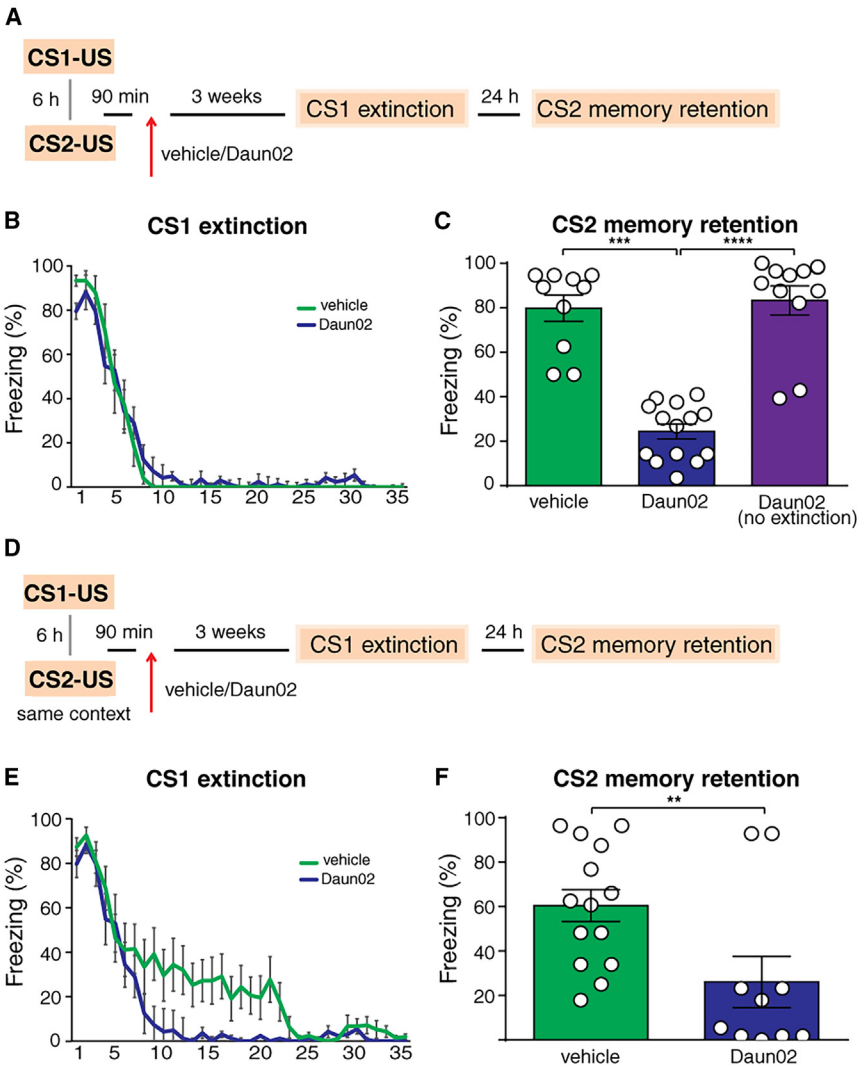

Figure 5. The dorsal hippocampus is necessary for the separation of temporally related remote memories

(A) Experimental design.

(B) Curves of fear extinction performed 3 weeks after learning in c-Fos-lacZ transgenic rats that received Daun02 (n = 14) or vehicle (n = 10).

(C) CS2 freezing is lower in Daun02- than in vehicle-injected rats and Daun02-injected rats where CS1 is not extinguished (n = 11) (Kruskal-Wallis and Dunn post hoc, H = 24.29, $p < 0.0001$).

(D) A similar experiment was repeated by presenting CS1 and CS2 in the same conditioning context.

(E) Curves of fear extinction performed 3 weeks after learning in c-Fos-lacZ transgenic (n = 10) and vehicle-injected (n = 14) rats that received the CS1-US and CS2-US pairings in the same conditioning cage.

(F) In rats that received CS1-US and CS2-US pairings in the same context, freezing to CS2 is lower in Daun02- than in vehicle-injected rats (Mann-Whitney, U = 25.50, p = 0.007).

Data are means ± SEM. *$p < 0.05$, **$p < 0.01$, ***$p < 0.001$, and ****$p < 0.0001$.

CS1 memory extinction (Figures 6F, S11B, and S11C), e.g., the decrease of freezing to CS2 was related to CS1 memory extinction. Combined, these data showed that both the dorsal hippocampus and the output pathway that exit from the ventral hippocampus are necessary for the segregation of remote memories.

Axons arising from hippocampal excitatory neurons synapse onto either excitatory or inhibitory neurons in the BLA.[35] Thus, the hippocampus might drive the separation of remote memories by directly recruiting GABAergic interneurons to the BLA. To test this possibility, we exploited the anterograde *trans*-synaptic properties of AAV1-Cre vectors to drive Cre-dependent transgene expression in postsynaptic neuronal targets from transduced presynaptic neurons.[36] We injected a Cre-dependent inhibitory DREADD (AAV1-hDlx-DIO-KORD-mCyRFP) vector into the BLA and a *trans*-synaptic AAV1-hSyn-Cre virus into the ventral hippocampus to drive their selective recombination in the BLA GABAergic cells receiving axons from the hippocampus (Figures 6G and 6H). Five weeks later, these viruses were selectively expressed in GABAergic BLA cells (Figures 6I and 6J), largely infecting PV cells (Figure 6J). Two groups of rats were injected with the two viruses in the hippocampus and BLA or with DIO-KORD-mCyRFP alone in the BLA. Both groups received salvinorin B[37] into the BLA (Figures 6K and S11D) 90 min after learning to inhibit GABAergic cells specifically receiving hippocampal projections. Three weeks later, CS1 memory was extinguished (Figure 6L), and CS2 memory was assessed. Compared to control rats, those injected with both viruses displayed lower freezing to CS2 (Figure 6M). Thus, direct projections from the hippocampus to the GABAergic interneurons within the BLA are necessary for segregating remote auditory fear memories.

DISCUSSION

This study provides insights into the neuronal processes that reduce the overlap between distinct but temporally related memories, such that related memories can be stored and retrieved independently.

Consistent with the memory allocation hypothesis,[10–13] we found that when two different fear events occurred closely in time, recent memories of those events shared overlapping neuronal populations in the BLA and were functionally linked. However, recalling or extinguishing one memory did not affect the recall or extinction of the other memory at later time points. Thus, remote memories of related events are functionally independent, ensuring memory specificity over time and preserving the integrity of one memory in case of modifications or disruption

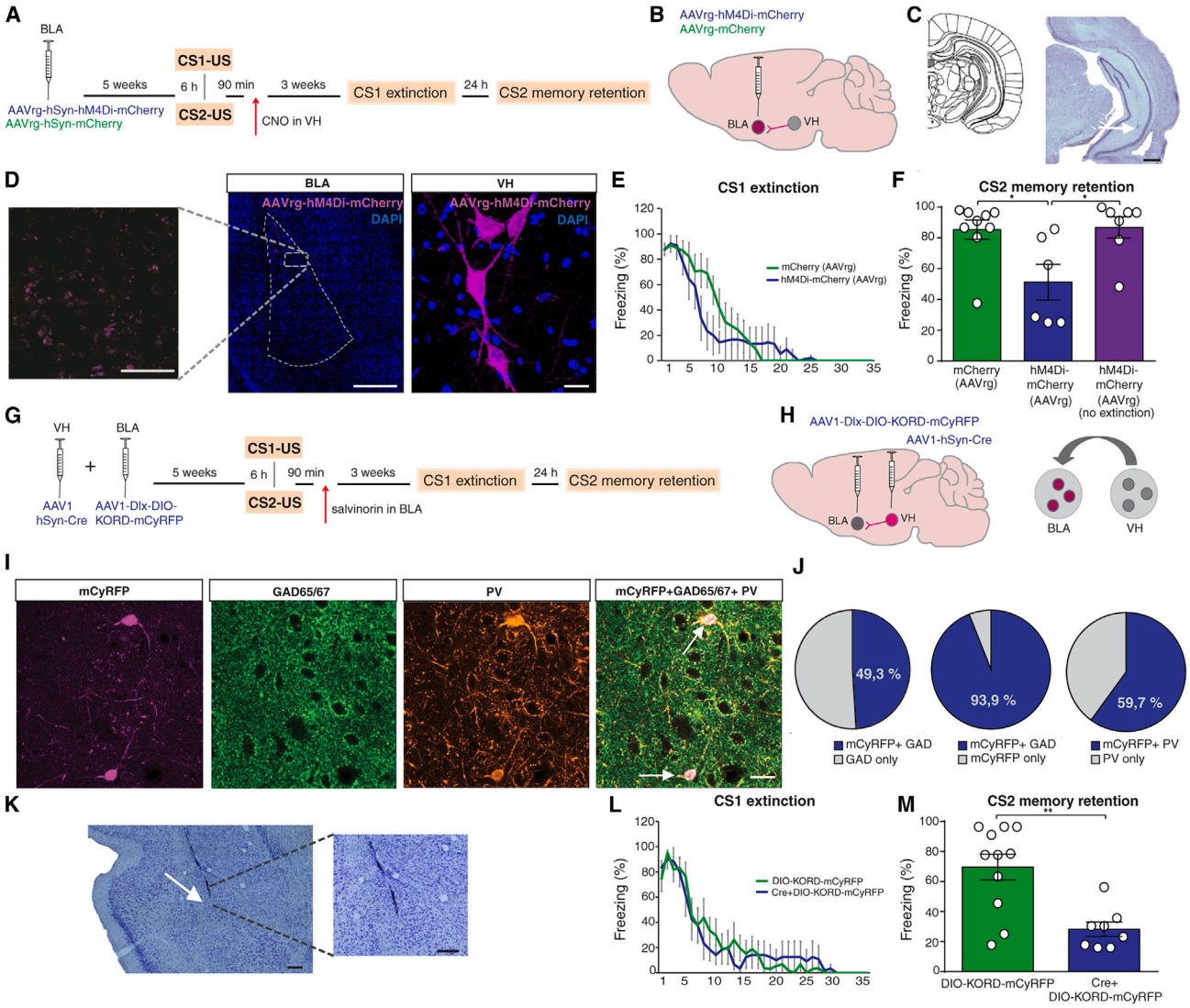

Figure 6. Excitatory hippocampal neurons that project to the BLA enable the separation of temporally related remote memories

(A) Experimental design.

(B) A retrograde AAVrg-hSyn-hM4D(Gi)-mCherry or a control retrograde AAVrg-hSyn-mCherry virus is infused into the BLA of wild-type rats.

(C) Clozapine-N-oxide (CNO) was injected into the ventral hippocampus. Scale bar, 1,000 μm (left). Plates were adapted from the Paxinos and Watson atlas (right).

(D) AAVs injected into the BLA (left; scale bars, 500 and 50 μm) are retrogradely transported toward cell bodies of the ventral hippocampus (right; scale bar, 20 μm).

(E) Curves of fear extinction performed 3 weeks after learning in the wild-type rats that received the retrograde AAVrg-hSyn-hM4D(Gi)-mCherry virus ($n = 6$) or AAVrg-hSyn-mCherry virus ($n = 9$) into the BLA.

(F) CS1 memory extinction decreases freezing to CS2 in AAVrg-hM4D(Gi)-mCherry rats compared with AAVrg-mCherry rats and AAVrg-hM4D-mCherry rats ($n = 7$) where CS1 is not extinguished ($H = 8.27$, $p = 0.016$).

(G and H) To label axons arising from the hippocampus and contacting the GABAergic cells in the BLA, we injected an AAV1-hSyn-Cre *trans*-synaptic vector in the hippocampus and an AAV1-hDlx-DIO-KORD-mCyRFP1 in the BLA of wild-type rats.

(I) Confocal images depict a selective recombination of AAV1-hSyn-Cre and AAV1-Dlx-DIO-KORD-mCyRFP in GAD^+ and PV^+ cells in the BLA. Scale bar, 20 μm.

(J) Five weeks after virus injections, 4 rats were submitted to the immunohistochemical analysis of virus expression, and the remaining control ($n = 11$) and AAV1-hSyn-Cre- and AAV1-Dlx-DIO-KORD-mCyRFP-injected ($n = 8$) rats were submitted to behavioral experiments. In the BLA, nearly half of GABAergic interneurons (GAD65/67-positive neurons) showed mCyRFP expression, and most neurons expressing mCyRFP were colabeled with GAD65/67 (left). Moreover, most neurons expressing mCyRFP were colabeled with PV (left).

(K) In the behavioral experiments, wild-type rats received the injection of salvinorin B (SalB; 3 μM) directly into the BLA 90 min after CS2-US pairing. Example of micrographs of the needle track in the BLA is shown. The higher magnification shows the absence of neuronal death after SalB injection. Scale bars, 200 μm.

(L) Curves of CS1 memory fear extinction performed 3 weeks after learning in both groups.

(M) After CS1 extinction, freezing to CS2 is lower in Cre+DIO-KORD-mCyRFP rats ($n = 8$) than in DIO-KORD-mCyRFP rats ($n = 11$) ($U = 10.50$, $p = 0.0039$).

Data are means ± SEM. $^*p < 0.05$ and $^{**}p < 0.01$.

of the other. At the neuronal level, the two remote memories mostly recruited distinct neuronal populations; however, they also shared a common neuronal population smaller than that of recent memories but significantly higher than that by chance. Common neuronal populations may capture shared features across related experiences.[12] Thus, common neuronal ensembles persisting across the two memories at remote time points may allow the maintenance of shared features of past experiences. Therefore, remote memories of two related events can maintain their specificity over time while retaining information about shared features from past experiences.

Numerous studies have implicated BLA PV neurons in fear learning.[32,38–40] Consistent with these findings, we observed an increase in activated PV-positive cells 90 min after learning in all conditioned groups, compared with naive rats, with a higher percentage of activated PV neurons in rats that learned two events in temporal proximity. Interestingly, the blockade of PV-containing neurons did not affect the retention of individual remote memory but disrupted the segregation of the two memories. This highlights the selective role of BLA PV cells in the consolidation of related remote fear memories. Notably, PV cells are required for the formation of separate remote memories as early as 90 min after learning, despite recent memories still being functionally linked 72 h after learning. Remote memories require cells that are generated or "tagged" shortly after learning.[41,42] PV cells may play a role in influencing these cells to form distinct remote memories.

Furthermore, the hippocampus sends axons that directly synapse onto GABAergic interneurons in the BLA, and blocking these axons prevents the formation of separate remote memories. The mentioned mechanism relies specifically on the segregation of remote memories but not on the formation of individual remote memories, highlighting an important distinction in the neural mechanisms underlying these processes. The hippocampus plays a vital role in managing highly related experiences through two processes: pattern separation and pattern competition.[1–7] Pattern separation reduces overlap among pieces of information to facilitate separate storage of this information, while pattern competition enables the recall of stored information from partial cues.[1–7] Our findings reveal a mechanism by which the hippocampus performs pattern separation, i.e., by directly activating BLA GABAergic interneurons. Consistent with this idea, human studies have also shown an interplay between the hippocampus and amygdala in the pattern separation of episodic and emotional memories.[14,15]

Alterations in neural mechanisms that underlie the distinction across highly similar memories to preserve memory specificity from interference are at the core of neuropsychiatric disorders, such as schizophrenia and PTSD. The hippocampus is particularly vulnerable to high-stress conditions, and, consequently, pattern separation processes may be compromised. Additionally, decreased GABA levels are associated with PTSD. Therefore, dysfunction in the neural processes we have described may contribute to the development of these disorders.

Limitations of the study

Experiments conducted with c-Fos-lacZ transgenic rats show a certain variability in behavior. This could be due to the fact that Daun02 might have destroyed a different percentage of neurons in different rats. To clarify this aspect, we analyzed the expression of β-gal in the remaining neurons and found no statistically significant differences between groups. However, it would be ideal to determine the direct correspondence between learned behavior and the number of neurons killed by Daun02. Such a measure, however, would likely not be accurate due to several factors, including the variability in the number of neurons activated prior to Daun02 administration. It is worth noting that despite this variability, the data obtained with c-Fos-lacZ transgenic rats show a clear statistical difference between groups, and these results have been fully confirmed with further experiments carried out by extinguishing mnemonic traces in wild-type animals, which did not receive any active compound.

Moreover, although we conducted chemogenetic experiments primarily targeting PV cells, we also utilized bicuculline—a selective inhibitor of overall GABAergic transmission—and a viral construct that infected PV cells as well as other GABAergic cells, such as somatostatin (SOM)-expressing cells. Therefore, we cannot rule out the possibility that additional GABAergic interneurons, aside from PV cells in the BLA, may contribute to the segregation of mnemonic traces. For example, recent findings have demonstrated that the modulation of the activity of SOM cells within the hippocampus can either promote or inhibit the formation of new fear memories.[43] A comparable mechanism may also be at play in the BLA to segregate fear memories. Subsequent studies are thus necessary to delve into this aspect further.

Finally, our study showed that besides the dorsal hippocampus, the output pathway that exits from the ventral hippocampus is also necessary for the segregation of remote memories. It could therefore be that the dorsal hippocampus processes the pattern separation of remote memories and, through the output pathway arising from the ventral hippocampus, regulates the separation of traces in target sites, such as the BLA. Alternatively, both dorsal and ventral regions of the hippocampus may be involved in the pattern separation process. Future studies will help distinguish between these possibilities.

STAR★METHODS

Detailed methods are provided in the online version of this paper and include the following:

- KEY RESOURCES TABLE
- RESOURCE AVAILABILITY
  - Lead contact
  - Materials availability
  - Data and code availability
- EXPERIMENTAL MODEL AND STUDY PARTICIPANT DETAILS
  - Animals
  - Behavioral procedures
- QUANTIFICATION AND STATISTICAL ANALYSIS

SUPPLEMENTAL INFORMATION

Supplemental information can be found online at https://doi.org/10.1016/j.celrep.2024.114151.

ACKNOWLEDGMENTS

We thank S. Ramirez (Dept. of Psychological and Brain Sciences, Boston, MA, USA) for the critical reading of the manuscript. We also thank S. Ramirez and S. Grella (Dept. of Psychological and Brain Sciences, Boston, MA, USA) for the kind gift of the AAV9-c-Fos-tTA and AAV9-TRE-EYFP viruses and G. Rainer (University of Fribourg, Switzerland) for providing PV-Cre transgenic rats. This work was supported by the Fondazione Cariverona (no. 2018.0780), CRT (2021.0485), Banca d'Italia (D63C23000630005), and Grant "Progetti di ricerca di Rilevante Interesse Nazionale (PRIN)" (20178NNRCR_002 and 2022BYZPFE) from the Italian Ministry of University and Research (MIUR).

AUTHOR CONTRIBUTIONS

G.C., A.R., and F.S. carried out and analyzed behavioral experiments; G.C., L.M., and E.M. performed immunohistochemical, immunofluorescent, and confocal microscopy analyses; and B.S. devised and analyzed the experiments and wrote the manuscript. All authors discussed the results and commented the manuscript.

DECLARATION OF INTERESTS

The authors declare no competing interests.

Received: May 24, 2023
Revised: February 21, 2024
Accepted: April 9, 2024

REFERENCES

1. Marr, D. (1971). Simple memory: a theory for archicortex. Phil. Trans. R. Soc. Lond. B *262*, 23–81.
2. Treves, A., and Rolls, E.T. (1994). Computational analysis of the role of the hippocampus in memory. Hippocampus *4*, 374–391.
3. McClelland, J.L., McNaughton, B.L., and O'Reilly, R.C. (1995). Why there are complementary learning systems in the hippocampus and neocortex: insights from the successes and failures of connectionist models of learning and memory. Psychol. Rev. *102*, 419–457.
4. O'Reilly, R.C., and Rudy, J.W. (2000). Computational principles of learning in the neocortex and hippocampus. Hippocampus *10*, 389–397.
5. Norman, K.A., and O'Reilly, R.C. (2003). Modeling hippocampal and neocortical contributions to recognition memory: A complementary-learning-systems approach. Psychol. Rev. *110*, 611–646.
6. Brady, T.F., Konkle, T., Alvarez, G.A., and Oliva, A. (2008). Visual long-term memory has a massive storage capacity for object details. Proc. Natl. Acad. Sci. USA *105*, 14325–14329.
7. Leal, S.L., and Yassa, M.A. (2018). Integrating new findings and examining clinical applications of pattern separation. Nat. Neurosci. *21*, 163–173.
8. Anacker, C., and Hen, R. (2017). Adult hippocampal neurogenesis and cognitive flexibility - linking memory and mood. Nat. Rev. Neurosci. *18*, 335–346.
9. Cayco-Gajic, N.A., and Silver, R.A. (2019). Re-evaluating Circuit Mechanisms Underlying Pattern Separation. Neuron *101*, 584–602.
10. Cai, D.J., Aharoni, D., Shuman, T., Shobe, J., Biane, J., Song, W., Wei, B., Veshkini, M., La-Vu, M., Lou, J., et al. (2016). A shared neural ensemble links distinct contextual memories encoded close in time. Nature *534*, 115–118.
11. Chowdhury, A., Luchetti, A., Fernandes, G., Filho, D.A., Kastellakis, G., Tzilivaki, A., Ramirez, E.M., Tran, M.Y., Poirazi, P., and Silva, A.J. (2022). A locus coeruleus-dorsal CA1 dopaminergic circuit modulates memory linking. Neuron *110*, 3374–3388.e8.
12. de Sousa, A.F., Chowdhury, A., and Silva, A.J. (2021). Dimensions and mechanisms of memory organization. Neuron *109*, 2649–2662.
13. Rashid, A.J., Yan, C., Mercaldo, V., Hsiang, H.L.L., Park, S., Cole, C.J., De Cristofaro, A., Yu, J., Ramakrishnan, C., Lee, S.Y., et al. (2016). Competition between engrams influences fear memory formation and recall. Science *353*, 383–387.
14. Leal, S.L., Noche, J.A., Murray, E.A., and Yassa, M.A. (2017). Age-related individual variability in memory performance is associated with amygdala-hippocampal circuit function and emotional pattern separation. Neurobiol. Aging *49*, 9–19.
15. Zheng, J., Stevenson, R.F., Mander, B.A., Mnatsakanyan, L., Hsu, F.P.K., Vadera, S., Knight, R.T., Yassa, M.A., and Lin, J.J. (2019). Multiplexing of Theta and Alpha Rhythms in the Amygdala-Hippocampal Circuit Supports Pattern Separation of Emotional Information. Neuron *102*, 887–898.e5.
16. Koya, E., Golden, S.A., Harvey, B.K., Guez-Barber, D.H., Berkow, A., Simmons, D.E., Bossert, J.M., Nair, S.G., Uejima, J.L., Marin, M.T., et al. (2009). Targeted disruption of cocaine-activated nucleus accumbens neurons prevents context-specific sensitization. Nat. Neurosci. *12*, 1069–1073.
17. Grosso, A., Cambiaghi, M., Renna, A., Milano, L., Roberto Merlo, G., Sacco, T., and Sacchetti, B. (2015). The higher order auditory cortex is involved in the assignment of affective value to sensory stimuli. Nat. Commun. *6*, 8886.
18. Grosso, A., Santoni, G., Manassero, E., Renna, A., and Sacchetti, B. (2018). A neuronal basis for fear discrimination in the lateral amygdala. Nat. Commun. *9*, 1214.
19. Lay, B.P.P., Koya, E., Hope, B.T., Esber, G.R., and Iordanova, M.D. (2023). The Recruitment of a Neuronal Ensemble in the Central Nucleus of the Amygdala During the First Extinction Episode Has Persistent Effects on Extinction Expression. Biol. Psychiatry *93*, 300–308.
20. Sacco, T., and Sacchetti, B. (2010). Role of secondary sensory cortices in emotional memory storage and retrieval in rats. Science *329*, 649–656.
21. Concina, G., Renna, A., Milano, L., and Sacchetti, B. (2022). Prior fear learning enables the rapid assimilation of new fear memories directly into cortical networks. PLoS Biol. *20*, e3001789.
22. Concina, G., Renna, A., Grosso, A., and Sacchetti, B. (2019). The auditory cortex and the emotional valence of sounds. Neurosci. Biobehav. Rev. *98*, 256–264.
23. Roy, D.S., Arons, A., Mitchell, T.I., Pignatelli, M., Ryan, T.J., and Tonegawa, S. (2016). Memory retrieval by activating engram cells in mouse models of early Alzheimer's disease. Nature *531*, 508–512.
24. Chen, B.K., Murawski, N.J., Cincotta, C., McKissick, O., Finkelstein, A., Hamidi, A.B., Merfeld, E., Doucette, E., Grella, S.L., Shpokayte, M., et al. (2019). Artificially Enhancing and Suppressing Hippocampus-Mediated Memories. Curr. Biol. *29*, 1885–1894.e4.
25. Zhang, X., Kim, J., and Tonegawa, S. (2020). Amygdala Reward Neurons Form and Store Fear Extinction Memory. Neuron *105*, 1077–1093.e7.
26. Han, J.H., Kushner, S.A., Yiu, A.P., Cole, C.J., Matynia, A., Brown, R.A., Neve, R.L., Guzowski, J.F., Silva, A.J., and Josselyn, S.A. (2007). Neuronal competition and selection during memory formation. Science *316*, 457–460.
27. McDonald, A.J. (1992). Cell types and intrinsic connections of the amygdala. In The Amygdala: Neurobiological Aspects of Emotion, Memory, and Mental Dysfunction (New York: Wiley), pp. 67–96.
28. McDonald, A.J., and Betette, R.L. (2001). Parvalbumin containing neurons in the rat basolateral amygdala: morphology and co-localization of calbindin-D (28k). Neuroscience *102*, 413–425.
29. Cohen, S.M., Ma, H., Kuchibhotla, K.V., Watson, B.O., Buzsáki, G., Froemke, R.C., and Tsien, R.W. (2016). Excitation-Transcription Coupling in Parvalbumin-Positive Interneurons Employs a Novel CaM Kinase-Dependent Pathway Distinct from Excitatory Neurons. Neuron *90*, 292–307.
30. Madsen, H.B., Guerin, A.A., and Kim, J.H. (2017). Investigating the role of dopamine receptor- and parvalbumin-expressing cells in extinction of conditioned fear. Neurobiol. Learn. Mem. *145*, 7–17.

31. Wright, A.M., Zapata, A., Hoffman, A.F., Necarsulmer, J.C., Coke, L.M., Svarcbahs, R., Richie, C.T., Pickel, J., Hope, B.T., Harvey, B.K., and Lupica, C.R. (2021). Effects of Withdrawal from Cocaine Self-Administration on Rat Orbitofrontal Cortex Parvalbumin Neurons Expressing *Cre recombinase*: Sex-Dependent Changes in Neuronal Function and Unaltered Serotonin Signaling. eNeuro *8*, 8.

32. Yau, J.O.Y., Chaichim, C., Power, J.M., and McNally, G.P. (2021). The Roles of Basolateral Amygdala Parvalbumin Neurons in Fear Learning. J. Neurosci. *41*, 9223–9234.

33. Ottersen, O.P. (1982). Connections of the amygdala of the rat. IV: Corticoamygdaloid and intraamygdaloid connections as studied with axonal transport of horseradish peroxidase. J. Comp. Neurol. *205*, 30–48.

34. Pitkänen, A., Pikkarainen, M., Nurminen, N., and Ylinen, A. (2000). Reciprocal connections between the amygdala and the hippocampal formation, perirhinal cortex, and postrhinal cortex in rat. A review. Ann. N. Y. Acad. Sci. *911*, 369–391.

35. Hübner, C., Bosch, D., Gall, A., Lüthi, A., and Ehrlich, I. (2014). Ex vivo dissection of optogenetically activated mPFC and hippocampal inputs to neurons in the basolateral amygdala: implications for fear and emotional memory. Front. Behav. Neurosci. *8*, 64.

36. Zingg, B., Chou, X.L., Zhang, Z.G., Mesik, L., Liang, F., Tao, H.W., and Zhang, L.I. (2017). AAV-Mediated Anterograde Transsynaptic Tagging: Mapping Corticocollicular Input-Defined Neural Pathways for Defense Behaviors. Neuron *93*, 33–47.

37. Marchant, N.J., Whitaker, L.R., Bossert, J.M., Harvey, B.K., Hope, B.T., Kaganovsky, K., Adhikary, S., Prisinzano, T.E., Vardy, E., Roth, B.L., and Shaham, Y. (2016). Behavioral and Physiological Effects of a Novel Kappa-Opioid Receptor-Based DREADD in Rats. Neuropsychopharmacology *41*, 402–409.

38. Windels, F., Crane, J.W., and Sah, P. (2010). Inhibition dominates the early phase of up-states in the basolateral amygdala. J. Neurophysiol. *104*, 3433–3438.

39. Wolff, S.B.E., Gründemann, J., Tovote, P., Krabbe, S., Jacobson, G.A., Müller, C., Herry, C., Ehrlich, I., Friedrich, R.W., Letzkus, J.J., and Lüthi, A. (2014). Amygdala interneuron subtypes control fear learning through disinhibition. Nature *509*, 453–458.

40. Lucas, E.K., Jegarl, A.M., Morishita, H., and Clem, R.L. (2016). Multimodal and site-specific plasticity of amygdala parvalbumin interneurons after fear learning. Neuron *91*, 629–643.

41. Lesburguères, E., Gobbo, O.L., Alaux-Cantin, S., Hambucken, A., Trifilieff, P., and Bontempi, B. (2011). Early tagging of cortical networks is required for the formation of enduring associative memory. Science *331*, 924–928.

42. Kitamura, T., Ogawa, S.K., Roy, D.S., Okuyama, T., Morrissey, M.D., Smith, L.M., Redondo, R.L., and Tonegawa, S. (2017). Engrams and circuits crucial for systems consolidation of a memory. Science *356*, 73–78.

43. Sharma, V., Sood, R., Khlaifia, A., Eslamizade, M.J., Hung, T.Y., Lou, D., Asgarihafshejani, A., Lalzar, M., Kiniry, S.J., Stokes, M.P., et al. (2020). eIF2α controls memory consolidation via excitatory and somatostatin neurons. Nature *586*, 412–416.

44. Ramirez, S., Liu, X., Lin, P.A., Suh, J., Pignatelli, M., Redondo, R.L., Ryan, T.J., and Tonegawa, S. (2013). Creating a false memory in the hippocampus. Science *341*, 387–391.

45. Paxinos, G., and Watson, C. (2007). The Rat Brain in Stereotaxic Coordinates (London: Academic Press Elsevier).

46. Ramanathan, K.R., Jin, J., Giustino, T.F., Payne, M.R., and Maren, S. (2018). Prefrontal projections to the thalamic nucleus reuniens mediate fear extinction. Nat. Commun. *9*, 4527.

47. MacLaren, D.A.A., Browne, R.W., Shaw, J.K., Krishnan Radhakrishnan, S., Khare, P., España, R.A., and Clark, S.D. (2016). Clozapine N-Oxide Administration Produces Behavioral Effects in Long-Evans Rats: Implications for Designing DREADD Experiments. eNeuro *3*.

48. Dickinson-Anson, H., and McGaugh, J.L. (1997). Bicuculline administered into the amygdala after training blocks benzodiazepine-induced amnesia. Brain Res. *752*, 197–202.

49. Ratano, P., Everitt, B.J., and Milton, A.L. (2014). The CB1 receptor antagonist AM251 impairs reconsolidation of pavlovian fear memory in the rat basolateral amygdala. Neuropsychopharmacology *39*, 2529–2537.

50. Xiu, J., Zhang, Q., Zhou, T., Zhou, T.T., Chen, Y., and Hu, H. (2014). Visualizing an emotional valence map in the limbic forebrain by TAI-FISH. Nat. Neurosci. *17*, 1552–1559.

STAR★METHODS

KEY RESOURCES TABLE

REAGENT or RESOURCE	SOURCE	IDENTIFIER
Antibodies		
chicken anti-Bgal	Aves Lab	Cat# BGL-1010 RRID:AB2313508
chicken anti-eYFP	Invitrogen	Cat#A10262; RRID: AB 2534023
rabbit anti-*c*-fos	Cell Signaling	Cat# 4384, RRID:AB2106617
mouse anti-CamKII	Merck	Cat # 05–532 RRID:AB309787
rat anti-*c*-fos	SySy	Cat# 226 017, RRID:AB_2864765
mouse anti-PV	Merck	Cat# P3088 RRID:AB_477329
guinea pig anti-PV	SySy	Cat# 195 004 RRID:AB_2156476
guinea pig anti-RFP	SySy	Cat# 390 005, RRID:AB2737051
rabbit anti-GAD65/67	Abcam	Cat# ab49832 RRID: AB_880149
Alexa Fluor 488 anti-chicken	Invitrogen	Cat#A11039; RRID: AB2534096
Cy3 anti-rabbit	Invitrogen	Cat #A10520, RRID:AB10563288
Cy5 anti-mouse	Invitrogen	Cat #A10524, RRID:AB2534033
Cy3 anti-rat	Invitrogen	Cat #A10522, RRID:AB2534031
Alexa Fluor 488 anti-guinea pig	Jackson	Cat # 106-545-003, RRID: AB_2337438
Cy3 anti-guinea pig	Jackson	Cat# 106-165-003, RRID: AB_2337423
Alexa Fluor 488 anti-rabbit	Invitrogen	Cat#A27034; RRID: AB2536097
DAPI	Merck	Cat #D9542
Bacterial and virus strains		
AAV9-*c*-fos-tTA	Steve Ramirez	N/A
AAV9-TRE-eYFP	Steve Ramirez	N/A
AAV5-hSyn-DIO-mCherry	Addgene	RRID: Addgene_ 50459
AAV5-hSyn-DIO-hM4D(Gi)-mCherry	Addgene Krashes et al. (2011)	RRID: Addgene_ 44362
AAVrg-hSyn- hM4D(Gi)-mCherry	Addgene	RRID: Addgene_ 50475
AAVrg-hSyn-mCherry	Addgene	RRID: Addgene_ 114472
AAV1-hDlx-DIO-KORD-mCyRFP	UZH	N/A
AAV1-hSyn-Cre	Addgene	RRID: Addgene_ 105553
Chemicals, peptides, and recombinant proteins		
Daun02	Hyculteh	HY-13061-5
Doxycycline chow	Bio-Serv	F5003
bicuculline methiodide	Tocris	2503/10
salvinorinB	Vinci Biochem	CAY-23582-25
CNO	Tocris	4936
Deposited data		
Raw data as supplementary file		N/A
Experimental models: Organisms/strains		
WT Sprague-Dawley rats	Internal facility	N/A
c-fos-lacZ Sprague-Dawley rats	Internal facility	N/A
PV-Cre Long Evans rats	G. Rainer	LE-Tg (Pvalb-iCre)
Software and algorithms		
Fiji	NIH	https://imagej.net/Fiji
Prism 9	GraphPad	https://www.graphpad.com/scientific-software/prism/
Graphic State	Coulbourne	N/A
SPSS 22	IBM	N/A

RESOURCE AVAILABILITY

Lead contact

Further information and request for resources and reagents should be directed to and will be fulfilled by the lead contact, Benedetto Sacchetti (benedetto.sacchetti@unito.it).

Materials availability

All materials generated in this study are available from the lead contact upon request.

Data and code availability

- All data reported are shared as raw data and are included as a supplementary file.
- This paper does not report original code.
- Any additional information required to reanalyze the data reported in this work paper is available from the lead contact upon request.

EXPERIMENTAL MODEL AND STUDY PARTICIPANT DETAILS

Animals

Healthy male rats (age, 65–70 days; weight, 240-350g) were housed in a plastic cage, 2–3 per cage, with food and water available *ad libitum*, under a 12 h light/dark cycle (lights on at 7:00 a.m.) at a constant temperature of 22 ± 1°C. All the experiments were conducted during the light phase of the day (8 a.m.–4 p.m.). Depending on experimental demands, Sprague-Dawley rats, c-fos-lacZ transgenic rats that had been bred for 35–40 generations on a Sprague-Dawley background, or Long-Evans transgenic rats expressing Cre recombinase under the rat parvalbumin (PV) promoter (LE-Tg (Pvalb-iCre), gifted by G. Rainer (University of Lausanne) were employed. Rats were derived from an internal animal facility breading. All the experiments were approved by the Italian Ministry of Health (authorization no. 408/2020-PR) and by the local bioethical committee of the University of Turin.

Behavioral procedures

Auditory fear learning tasks

Rats were gently taken from their home cage and carried from the housing room to the soundproofed room. Once there, animals were placed inside the conditioning apparatus consisting of a rectangular black cage (32 × 40 × 30cm) equipped with a stainless-steel rods grid (1 cm in diameter, spaced 1.5 cm apart) connected to a shock delivery set-up. Rats were left undisturbed for 1 min. After this time, conditioned stimuli consisting of a pure tone of 15-kHz of frequency (15 s of duration each, 80 dB, 36 s inter-trials interval, ITI) were administered and acted as CS1 in most experiments. The last 1 s of each tone was paired with a painful unconditioned stimulus (US, 0.5 mA, 1 s). Immediately (0-min group), 6 h (6-h group) or 7 days (7-day group) later, rats were submitted to another round of fear learning.[21] They were presented with conditioned stimuli acting as CS2 and consisting of pure tones of 1-kHz of frequency (8s, 80 dB, 22s ITI). The last 1 s of each tone was paired with a painful unconditioned stimulus (US, 0.5 mA, 1 s).

In the 0-min group, CS1-US and CS2-US pairings occurred consecutively within the same conditioning cage (context A). Rats underwent 4 CS1-US pairings immediately followed by 3 CS2-US pairings, resulting in a total of 7 CS-US pairings. In cases where the experimental requirements dictated (as in the experiments depicted in Figures 4A–4C), the 7 CS-US pairings were repeated twice with a 6-h interval. In the 6-h and 7-day groups, rats experienced 7 CS1-US and 7 CS2-US. The two pairings occurred in a distinct conditioning cage (context B) to further differentiate the two events. The two pairings were separated by either a 6-h interval in the 6-h group or a 7-day interval in the 7-day group. The cage consisted of a skinner box module.[17–21] Animals were carried in two different buckets to the two conditioning chambers. At the end of the conditioning sessions, they were brought back to their home cage.

In the counterbalanced experiments, CS1 consisted of pure tones of 1-kHz of frequency, 8 s of duration each, 80 dB, 22s ITI, and CS2 consisted of pure tones of 15-kHz, 15s, 80dB, 36s ITI.

Memory tests and extinction trials

Animals were transported singularly from the facility to the experimental rooms within small transparent buckets. Depending on the experimental demand, 72 h or 3 weeks after auditory fear learning trials, rats were submitted to:

CS1 memory reactivation and CS2 memory test in the c-fos-lacZ transgenic rats (Figure 1, and 4L)

In c-fos-lacZ transgenic rats, CS1 memory was reactivated at recent or remote time points by presenting 4 CS1 (pure tone of 15-kHz, 15 s, 80 dB, 36 s ITI) identical to those employed during CS1-US pairing. To selectively trigger the reactivation of CS1 memory while minimizing interference associated with contextual cues,[17–21] CS1 was presented in a novel environment (context C). Ninety min later, rats received Daun02 or vehicle administration. CS2 memory was tested 3 days later in a totally new cage (context D), consisting of a transparent plastic cage with a black painted side. The cage was enclosed within a sound-attenuating box equipped with an exhaust fan, which eliminated odorized air from the enclosure and provided background noise of 60 dB. Animals were allowed to explore the cage for 5 min during the habituation session. The following day, after 2 min of free exploration, rats were presented with 7

CS2 (1 kHz, 8 s, 22 ITI) identical to those employed during CS2-US pairing. Three days after CS2 memory retention test, CS1 memory retention was tested by presenting 4 CS1 (15-kHz, 15 s, 80 dB, 36 s ITI) in another different cage (context E, 26 × 36 × 25cm) with black painted stripes on the walls.

CS1 memory extinction and CS2 memory retention test in Sprague-Dawley rats (Figures 2 and 4I–4K, and 6), c-fos-lacZ transgenic rats (Figure 5), and PV-Cre rats (Figures 4F–4H)

To extinguish CS1 memory, rats were put in a new apparatus consisting of a transparent plastic cage with a black painted side and enclosed within a sound-attenuating box equipped with an exhaust fan, which eliminated odorized air from the enclosure and provided background noise of 60 dB. Rats were left undisturbed for 2 min. Then, 35 CS1 identical to those employed during CS1-US pairing (e.g., a pure tone of 15-kHz, 15 s, 80 dB) were delivered at 50 s ITI in the absence of any USs, for a total duration of 30 min. The subsequent day, CS2 memory retention was tested by presenting 7 CS2 (pure tones of 1-kHz, 8s, 80 dB, 22 s ITI) identical to those employed during CS2-US pairing.

In the experiments where CS1 memory extinction was replaced by CS1 memory test, rats were presented only with 4 CS1 (15-kHz, 15 s, 80 dB, 36 s ITI).

CS1 and CS2 memory test in Sprague-Dawley rats injected with the virus cocktail of AAV9-*c*-fos-tTA and AAV9-TRE-eYFP viruses (Figure 3)

To label neurons activated during CS1 and CS2 memory recall, we injected an inducible, activity-dependent virus cocktail of AAV9-*c*-fos-tTA and AAV9-TRE-eYFP viruses, which labeled neurons expressing the immediate-early gene c-fos in a doxycycline (Dox)-dependent manner.[23,24] Rats were placed on a diet containing 40 mg/kg doxycycline (Dox) for 5 days before receiving viruses' injections with access to food and water *ad libitum*. Rats were kept on this diet up to 48 h before CS1 memory test, which occurred at recent or remote time points. Fourth-8 h before CS1 memory test, rats were habituated for 5 min to the two new cages where CS1 and CS2 memories will be tested. One cage consisted of a transparent plastic cage with a black painted side enclosed within a sound-attenuating box equipped with an exhaust fan. The other cage consisted of a rectangular cage (26 × 36 × 25cm) with black-painted stripes on the walls.

Six hours after the habituation sessions, the Dox-containing diet was replaced with standard rats' chow (*ad libitum*) to open a time window of activity-dependent labeling.[24,44] Fourth-8 h later, CS1 memory was retrieved by presenting 4 CS1 (15-kHz, 15 s, 80 dB, 36 s ITI) identical to those employed during CS1-US pairing. Following behavioral tagging, rats were returned to their home cage and were put again on the Dox diet. Twenty-four hours later, CS2 memory was retrieved by presenting 7 CS2 (pure tones of 1-kHz, 8s, 80 dB, 22 s ITI) identical to those employed during CS2-US pairing. Ninety min later, rats were intracardially perfused.

Freezing measure. In all experimental procedures, the assessment of the fear memory retention was determined as a freezing response, analyzed as the complete absence of somatic mobility except for respiratory movements. For each animal, the amount of time (in seconds) spent in freezing was measured offline by two independent observers who were blinded to the animal groups.

Surgical procedures

To administer active compounds or viruses in the target brain sites, rats were anesthetized with isoflurane: the induction was performed at 4% [v/v] in 2 L/min medical air and extended to a continuous exposure at 2% [v/v]) when rats were mounted in the stereotaxic apparatus.

Each rat was operated separately. Animals belonging to the active compounds or saline/vehicle groups were manipulated in an interleaved way. An incision of the skull was made, and small burr holes were drilled to allow the penetration of a 28-gauge infusion needle. A 10 μL Hamilton syringe mounted on an infusion pump was used to deliver substances. The substances were bilaterally injected at a rate of 0.3 μL/min at the following stereotaxic coordinates taken from Paxinos and Watson atlas[45]:

Basolateral amygdala (BLA): AP: −2.4 L: ±5.5 DV: −8.3 and AP: −3.4 L: ±5.5 DV: −8.3.

Secondary Auditory Cortex (Te2): AP: −5,8 L: ±7,2 DV: −6.0 and AP: −6,8 L: ±7,2 DV: −6.0.

Dorsal Hippocampus: AP: −2.8 L: ±1.6 DV: −3.5 and AP: −4.2 L: ±2.6 DV: −3.5.

Ventral Hippocampus: AP: −5.0 L: ±5.0 DV: −6.0 and AP: −6.0 L: ±5.0 DV: −6.0.

The needle was left in place for 3 min in the case of the active compounds' injection or 5 min in the case of the viruses' injection. The incision was then closed with stainless steel wound clips. The animal was given a subcutaneous (s.c.) injection of the analgesic/anti-inflammatory ketoprofen (2 mg/kg body weight) and kept warm and under observation until recovery from anesthesia.

At the end of the experiments, needle track placement was verified in Nissl-stained sections. The sections were histologically verified under a microscope magnified at 2.5×.

The following specific surgical procedures were employed depending on the experimental demand:

Daun02 injection into BLA (Figures 1 and 4L), Te2 (Figure S7), Dorsal Hippocampus (Figure 5)

For the treatment of c-fos-lacZ transgenic rats, Daun02 was dissolved to a final concentration of 5 mg/ml in a solution of 10% DMSO, 6% Tween-80, and 84% phosphate-buffered saline.[17,18] As in these studies,[17,18] a volume of 1μL of Daun02 or vehicle was injected per site in BLA, Te2, or Dorsal Hippocampus at the above stereotaxic coordinates.

AAV9-*c*-fos-tTA and AAV9-TRE-eYFP viruses' injection into BLA (Figure 3)

To label neurons activated by memory processes, a cocktail (1:1 ratio) of AAV9-*c*-fos-tTA (3 x 10^13 GC/mL) and AAV9-TRE-eYFP (1.2 x 10^13 GC/mL)[23,24] was injected into BLA at the above stereotaxic coordinates at the volume of 0.8 μL per site. Viruses were gifted by S. Ramirez (Boston University).

AAV5-hSyn-DIO-hM4D(Gi)-mCherry injection into BLA of PV-Cre rats and CNO i.p. injections (Figures 4A–4H)

To block parvalbumin (PV)-expressing cells within BLA, the AAV5-hSyn-DIO-hM4D(Gi)-mCherry (2.4 x 10^13 GC/mL) and control virus (AAV5-hSyn-DIO-mCherry, 2.1 x 10^13 GC/mL)(Addgene) were injected into BLA at the above stereotaxic coordinates at the volume of 0.8 μL per site. Fear learning trials occurred three weeks following viruses' injections. Clozapine-N-Oxide (CNO) (3 mg/kg, in saline solution) was injected intraperitoneally (i.p.) 60 min after CS2-US pairing. The dosage[46] and time of injection[47] were chosen based on previous studies in rats. In rats, levels of CNO peak at 30 min and decline to low levels by 6 h after injection.[47]

Bicuculline injection into BLA (Figures 4I–4L)

To block GABAergic neurotransmission, GABAA antagonist (−)-bicuculline methiodide was dissolved in saline at the dosage of 50 ng per 0.5 μL per side. The dosage was chosen based on previous studies[48,49] showing no effects on fear behavior and fear memory by itself. According to those studies,[48,49] a volume of 0.5 μL or saline was injected in BLA, at the stereotaxic coordinate of AP: −2.8 L: ±5.5 DV: −8.0.

AAVrg-hSyn-hM4D(Gi)-mCherry vector injection into BLA and CNO injection into the ventral hippocampus (Figures 6A–6F)

To inactivate hippocampal excitatory terminals in the BLA, rats were injected with the retrograde AAVrg-hSyn-hM4D(Gi)-mCherry vector (2.4 x 10^13 GC/mL) into BLA at the volume of 0.8 μL per site at the above stereotaxic coordinates. A control group received the AAVrg-hSyn-mCherry virus (2.0 x 10^13 GC/mL). All vectors were purchased from Addgene. Five weeks later, rats were submitted to fear learning. Ninety min later, CNO was administered into the ventral hippocampus of PV-Cre rats at the volume of 0.8 μL per site at the above stereotaxic coordinates.

AAV1-hDlx-DIO-KORD-mCyRFP and AAV1-hSyn-Cre injection and SalvinorinB injection (Figures 6G–6M)

To manipulate inhibitory interneurons of BLA that are directly contacted by hippocampal axons, we injected an inhibitory Cre-dependent inhibitory DREADD (AAV1-hDlx-DIO-KORD-mCyRFP) vector (University of Zurich, UZH, VVF), in BLA (4.8 x 10^12 GC/mL) at the volume of 0.8 μL per site at the above stereotaxic coordinates. In the meantime, a *trans*-synaptic Cre (AAV1-hSyn-Cre) (2.1 x 10^13 GC) virus (Addgene), was injected in the ventral hippocampus at the volume of 1.0 μL per site at the above stereotaxic coordinates. The control group received only the AAV1-hDlx-DIO-KORD-mCyRFP) vector into the BLA but not the AAV1-hSyn-Cre virus into the ventral hippocampus. Five weeks later, rats were conditioned to the two auditory fear events. Ninety min later, they received salvinorinB (SalB)[37] into BLA to inhibit GABAergic cells specifically receiving hippocampal projections. SalB was dissolved in saline (3 μM), and directly injected into BLA 90 min after CS2-US learning. SalB was injected into BLA at a volume of 0.5 μL per site with the following stereotaxic coordinates: AP: −2.8 L: ±5.5 DV: −8.0.

Immunohistochemistry

Rats were deeply anesthetized and perfused intracardially with 4% PAF. Brains were dissected, stored overnight at 4°C, and finally transferred to 30% sucrose. Coronal sections (35 μm) were cut on a cryostat and collected in PBS and incubated in a blocking solution for 1 h at RT.

To analyze the expression of the β-gal as an indicator of neuronal activity-induced activation and verify the effectiveness of the Daun02 procedure, sections were incubated in primary chicken anti-Beta Gal (1:1000, Aves Lab) antibodies in the blocking solution overnight at RT. Subsequently, sections were washed with PBS and incubated for 1 h at RT with secondary fluorescent Alexa Fluor 488 anti-chicken (1:1000, Invitrogen) antibody diluted in PBS.

To analyze cells activated by CS1 or CS2 or both memories, sections were incubated in primary chicken anti-eYFP (1:5000, Invitrogen), rabbit anti-*c*-fos (1:2000, Cell Signaling), mouse antibody anti-CamKII (1:500 dilution, Merck) antibodies in the blocking solution overnight at RT. Subsequently, sections were washed with PBS and incubated for 1 h at RT with secondary fluorescent Alexa Fluor 488 anti-chicken (1:1000, Invitrogen), Cy3 anti-rabbit (1:1000, Invitrogen) and Cy5 anti-mouse (1:1000, Invitrogen) antibodies diluted in PBS.

To analyze c-fos and Parvalbumin (PV) positive cells, sections were incubated with rat anti-*c*-fos (1:2000, SySy) and mouse anti-PV (1:2000, Merck) antibodies and subsequently with secondary Cy3 anti-rat (1:1000, Invitrogen) and Cy5 anti-mouse (1:1000, Invitrogen) antibodies diluted in PBS. All sections were then stained with DAPI, and cover slipped.

To analyze the diffusion of AAV5-DIO-hM4D(Gi)-mCherry and AAVrg-hM4D(Gi)-mCherry vectors (and their AAV controls), mCherry expression was visualized without any amplification. In PV-Cre rats expressing DIO-hM4D(Gi)-mCherry, sections were incubated with guinea pig anti-PV (1:2000, SySy) antibody and Alexa Fluor 488 anti-guinea pig (1:1000, Jackson) secondary antibody.

In the KORD-dependent chemogenetic approach, AAV1-hSyn-Cre and AAV1-Dlx-DIO-KORD-mCyRFP1 recombination in BLA neurons receiving direct projections from the ventral hippocampus was examined through mCyRFP1 amplification. Sections were incubated in a blocking solution for 1 h at RT and then, in primary polyclonal guinea pig anti-RFP (1:500, SySy), and rabbit anti-GAD65/67 (1:1000 dilution, Abcam), and mouse anti-PV (1:2000, Merck) in the blocking solution overnight at RT. Subsequently, sections were washed with PBS and incubated for 1 h at RT with secondary fluorescent Cy3 anti-guinea pig (1:1000, Jackson), Alexa Fluor 488 anti-rabbit (1:1000, Invitrogen) and Cy5-anti mouse (1:1000, Invitrogen) antibodies diluted in PBS. All sections were stained with DAPI, and cover slipped.

Microscopy and cell counts

Cellular markers, viral fluorophores of chemogenetic and control vectors were visualized by a Zeiss Airyscan confocal microscope. Tissues were imaged using four lasers (405, 488, 568, and 640 nm), each corresponding this time to the peak emission spectrum for DAPI (Nissl stain for cell nuclei); Alexa Fluor 488; mCherry, mCyRFP, Cy3; and Cy5, respectively.

In most cases (analysis of cells infected AAV9-*c*-fos-tTA and AAV9-TRE-eYFP, AAV5-hSyn-DIO- hM4D(Gi)-mCherry and its AAV control, c-fos, and PV quantification, analysis of retrograde labeled hippocampal cells and KORD-expressing BLA neurons) images

were acquired at a 40× objective using a stack of 15 sections, spaced 1.5 μm apart (159 μm square; zoom fraction, 1.0). For AAVrg-hSyn-hM4D(Gi)-mCherry, micrographs of BLA were acquired as mosaic images, with each individual image acquired as a z stack of 10 sections, spaced 1.5 μm apart (159 μm square; zoom fraction, 1.0) by using a 40× objective.

Cell counts were performed in the BLA region at the anteroposterior (AP) coordinates ranging from 2.4 to 3.5 mm from the bregma.[45] Only putative neurons were included in the analysis, and glial cells, identified from their small size (~5μm diameter) and bright, uniform nuclear counterstaining, were excluded.

eYFP$^+$, c-fos$^+$ and eYFP$^+$c-fos$^+$ cells count

The number of excitatory neurons expressing eYFP (eYFP$^+$), c-fos (c-fos$^+$) or both (eYFP and c-fos overlap; eYFP$^+$c-fos$^+$) were normalized on DAPI-positive cells. Neurons activated by the CS1 presentation minus those activated also during the CS2 presentation were calculated as total eYFP$^+$cells minus eYFP$^+$c-fos$^+$cells and were referred to as neurons activated only by CS1 (eYFP$^+$CS1). Neurons activated by the only CS2 presentation were calculated as total c-fos$^+$cells minus eYFP$^+$c-fos$^+$cells and were referred to as c-fos$^+$CS2 neurons.

The chance level for each neuron to be eYFP and c-fos double-positive was calculated as [(eYFP$^+$c-fos$^-$/DAPI) × (eYFP$^-$c-fos$^+$/DAPI)],[10,18,24,50] and the predicted overlap was: [(eYFP$^+$c-fos$^-$/DAPI) × (eYFP$^-$c-fos+/DAPI)] × DAPI.

The reactivation ratio (RRI) was calculated as the ratio of eYFP and c-fos double-positive cells (eYFP$^+$c-fos$^+$) among all c-fos positive cells: eYFP$^+$c-fos$^+$/c-fos$^+$cells. Thus, the RRI predicted by chance was equal to the predicted overlap divided by all c-fos$^+$ cells[18,50].

The observed overlap and the overlap expected by chance, as well as the predicted and the observed RRI of each group, were compared using a Student's two-tailed paired t test. To test the difference between groups, we used a Student's two-tailed unpaired t test.

c-fos$^+$, PV$^+$ and c-fos$^+$PV$^+$ cells count

The number of cells expressing c-fos, PV, and double-positive (c-fos and PV overlap) were quantified for each animal. c-fos positive cells were normalized on the total number of DAPI cells, while double-positive cells (c-fos and PV overlap) were normalized on the total number of PV cells. Data collected from each section were then averaged to produce the mean of each animal and the results were statistically compared.

QUANTIFICATION AND STATISTICAL ANALYSIS

Animals from the same brood were *a priori* randomly assigned to each experimental group, in a weight-balanced manner. The sample size estimation for each group was based on effect size calculation, on similar works in the field and on the previous laboratory experience. Inclusion/exclusion criteria were based on histological assessments. All experiments were conducted in at least two biological replicates.

The Kolmogorov-Smirnov test was used to determine whether the data were normally distributed. When data were normally distributed, data from two groups were compared using two-tailed unpaired Student's t-tests. Multiple-group comparisons were assessed using a one-way ANOVA with Tukey's post-hoc test.

When data were non-normally distributed, they were analyzed using the Mann-Whitney test to test the differences between two different groups. Multiple-group comparisons were assessed using Kruskal-Wallis test with Dunn post-hoc test.

To determine whether the data met the assumptions of the statistical approach, we rejected the null hypothesis at the $p < 0.05$ level. All statistical analyses were performed using SPSS Statistics 22 (IBM). The statistical parameters (i.e., the exact value of *n* for each experimental group of animals, SEM, the statistical test, and the exact *p* value) were reported in the legends. All data were presented as mean ± SEM.